Published in final edited form as:

Oral Oncol. 2014 December ; 50(12): 1149–1156. doi:10.1016/j.oraloncology.2014.09.013.

Wild-type p53 reactivation by small-molecule Minnelide™ in human papillomavirus (HPV)-positive head and neck squamous cell carcinoma

Emiro Caicedo-Granados[a], **Rui Lin**[a], **Caitlin Clements-Green**[a], **Bevan Yueh**[a], **Veena Sangwan**[b], and **Ashok Saluja**[b]

[a]Department of Otolaryngology—Head and Neck Surgery, University of Minnesota

[b]Department of Surgery, University of Minnesota

Abstract

Objectives—The incidence of high-risk human papillomavirus (HR-HPV) head and neck squamous cell carcinoma (HNSCC) continues to increase, particularly oropharyngeal squamous cell carcinoma (OPSCC) cases. The inactivation of the p53 tumor suppressor gene promotes a chain of molecular events, including cell cycle progression and apoptosis resistance. Reactivation of wild-type p53 function is an intriguing therapeutic strategy. The aim of this study was to investigate whether a novel compound derived from diterpene triepoxide (Minnelide™) can reactivate wild-type p53 function in HPV-positive HNSCC.

Materials and Methods—For all of our in vitro experiments, we used 2 HPV-positive HNSCC cell lines, University of Michigan squamous cell carcinoma (UM-SCC) 47 and 93-VU-147, and 2 HPV-positive human cervical cancer cell lines, SiHa and CaSki. Cells were treated with different concentrations of triptolide and analyzed for p53 activation. Mice bearing UM-SCC 47 subcutaneous xenografts and HPV-positive patient-derived tumor xenografts were treated with Minnelide and evaluated for tumor growth and p53 activation.

Results—In HPV-positive HNSCC, Minnelide reactivated p53 by suppressing E6 oncoprotein. Activation of apoptosis followed, both in vitro and in vivo. In 2 preclinical HNSCC animal models (a subcutaneous xenograft model and a patient-derived tumor xenograft model), Minnelide reactivated p53 function and significantly decreased tumor progression and tumor volume.

Corresponding Author: Emiro Caicedo-Granados, MD, 420 Delaware St SE, MMC 396, Minneapolis, MN 55455, caic0001@umn.edu, 612-625-3200, Fax: 612-625-2101.

Suggestions for Reviewers: John Lee, MD: John.Lee@SanfordHealth.org, Paul Harari, MD: harari@humonc.wisc.edu, Eva Szabo, MD: szaboe@mail.nih.gov

Conflict of Interest Statement: Emiro Caicedo-Granados, MD Nothing to disclose
Rui Lin, PhD Nothing to disclose
Caitlin Clements-Green Nothing to disclose
Bevan Yueh, MD Nothing to disclose
Veena Sangwan, PhD Nothing to disclose
Ashok Saluja, PhD The University of Minnesota has filed a patent for Minnelide™ (which has been licensed to Minneamrita Therapeutics LLC, Moline, IL). Ashok Saluja has a financial interest in this company and is one of the inventors on this patent.

Conclusion—Triptolide and Minnelide caused cell death in vitro and in vivo in HPV-positive HNSCC by reactivating wild-type p53 and thus inducing apoptosis. In addition, in 2 HPV-positive HNSCC animal models, Minnelide decreased tumor progression and induced apoptosis.

Keywords

Minnelide; HPV; oropharyngeal cancer; preclinical animal model; p53 reactivation

Introduction

In the United States alone, the incidence of human papillomavirus (HPV)-positive oropharyngeal squamous cell carcinoma (OPSCC) dramatically increased from 1988 to 2004: by 225%. If this rate of growth were to continue, the annual number of HPV-positive OPSCC cases would surpass the annual number of cervical cancer cases by 2020.[1] Part of the explanation for this increase is the high prevalence, about 7%, of oral HPV infection among men and women ages 14 to 69 years. About 1% of them (an estimated 2.13 million individuals) are infected with high-risk HPV 16.[2]

The prognosis for patients with HPV-positive OPSCC is better than for those with cancers caused by more traditional risk factors, such as tobacco use and alcohol abuse. Still, patients with HPV-positive OPSCC experience severe toxicity under current forms of treatment. No agents that reactivate wild-type p53 are available to treat OPSCC, but the development of such an agent would likely augment the effectiveness of treatment and potentially reduce the side effects of current chemotherapy and radiation regimens.

Triptolide, a diterpene triepoxide derivative from the Chinese herb *Tripterygium wilfordii*, has been used for centuries as a medicinal plant. It has shown success in the clinical treatment of patients with rheumatoid arthritis and autoimmune disease and as an antirejection agent for organ transplant recipients.[3] In recent years, triptolide's strong antiproliferative activity and ability to induce apoptosis have been demonstrated in an extensive range of cancers in vitro and in vivo.[4-8]

Investigators at the University of Minnesota have developed a highly water-soluble analog of triptolide (Minnelide™). In animal models of pancreatic cancer,[9] Minnelide has been shown to decrease tumor burden, morbidity, and locoregional spread and to increase overall survival. It is now the focus of a phase 1 clinical trial for patients with gastrointestinal malignancies.[10] Our initial work suggests that Minnelide may have a significant effect on HPV-positive OPSCC; we have been particularly interested in determining its mechanism of action.

High-risk oncogenic HPV 16 and 18 are capable of transforming epithelial cells from both the genital tract and the upper respiratory tract.[11] The transforming potential of high-risk HPV is due to the effects of 2 viral oncoproteins, E6 and E7, which functionally inactivate 2 tumor suppressor proteins: p53 (by E6) and pRB (by E7). Expression of E6 and E7 results in cellular proliferation, loss of cell cycle regulation, impaired cellular differentiation, and chromosomal instability.[12] Unlike HPV-negative head and neck squamous cell carcinoma (HNSCC), where the P53 gene is inactivated by irreversible mutations, HPV-positive

HNSCC uniquely harbors an inactivated wild-type P53 gene. If inactivation of p53 by E6 is indispensable for HPV-mediated tumorigenesis, reactivation of p53 could be a logical strategy to eliminate HPV-positive carcinoma cells.

The aim of this study was to investigate whether Minnelide can reactivate wild-type p53 function in HPV-positive HNSCC.

Materials and Methods

Cell lines and reagents

We obtained 2 head and neck cancer cell lines derived from HPV 16-positive head and neck tumors: University of Michigan squamous cell carcinoma (UM-SCC) 47 (from Dr Thomas Carey, University of Michigan) and 93-VU-147 (from Dr John Lee, Sanford Health South Dakota). In addition, we purchased 2 HPV 16-positive human cervical cancer cell lines, SiHa and CaSki, from the American Type Culture Collection (ATCC). We maintained UM-SCC 47, 93-VU-147, and SiHa cells in Eagle's minimal essential medium and CaSki in 1640 Roswell Park Memorial Institute (RPMI) medium; the medium for all 4 cell lines was supplemented with 10% fetal bovine serum, L-glutamine (5.8 mg/ml), and penicillin/streptomycin (50 μg/ml), as adherent monolayer cultures, at 37°C in 5% CO_2.

We purchased human epidermal keratinocytes (HEKs) from Lifeline Cell Technology (Frederick, MD) and maintained them, as monolayer cultures, on DermaLife K Medium complete kit.

We also obtained an HPV-negative head and neck carcinoma cell line, UM-SCC 11A (again, from Dr Thomas Carey, University of Michigan), and maintained those cells in Eagle's minimal essential medium.

All the cell lines we used were tested and found to be mycoplasma-free.

In vitro cell proliferation assay

We plated UM-SCC 47, 93-UV-147, and SiHa cells at a density of 7.5×10^3 per well in 96-well plates. After 48 hours, cells were incubated with dimethyl sulfoxide (DMSO), Taxol (40 ηM), cisplatinum 5μM, and triptolide concentrations (range, 25-100 ηM) for 24 and 48 hours. Cell viability was determined via 3-(4,5-dimethyl-2-thiazolyl)-2,5-diphenyl-2H-tetrazolium bromide (MTT) assay (Sigma, St Louis, MO), with cells incubated for 4 hours in medium containing MTT, and via cell counting kit-8 (Dojindo Molecular Technologies Inc, Japan), per the manufacturer's instructions. Mitochondrial dehydrogenases of live cells converted MTT to a water-insoluble purple formazan, which we then solubilized via lysis buffer. Absorbance was read at 560 nm on a 96-well microtiter plate reader.

Caspase 3/7 assay

To analyze caspase-3/7 activity, we used the Caspase-Glo luminescent assays (Promega, Madison, WI), per the manufacturer's instructions. Cells (1×10^4) were seeded into 96-well white opaque plates and into a corresponding optically clear 96-well plate, then allowed to adhere overnight. The next day, cells were treated with 50 ηM of staurosporine (STS) as a

positive control and with varying concentrations of triptolide for 24 and 48 hours. At the end of the incubation time, 100 μL of the appropriate Caspase-Glo reagent was added to each well containing 100 μL of blank, negative control, or treated cells in culture medium. Plates were gently mixed and incubated for 1 hour at room temperature. The luminescence was then read in a luminometer. The corresponding 96-well clear plate was used to measure the number of viable cells with the CCK-8 reagent. Caspase activity was normalized to those values.

Transient transfection and luciferase reporter gene assays

The p53-Luc reporter construct containing the promoter-binding site upstream of firefly luciferase has been previously described.[13] The pCMV-Lac-Z reporter construct (β-gal) was a generous gift from Dr Richard Pestell, Georgetown University. Cell cultures at 70% confluence were cotransfected with appropriate luciferase reporter plasmid (2 μg/well) and with the pCMV-Lac-Z reporter construct (0.4 μg/well) to correct for transfection efficiency in Opti-MEM medium containing 10 μg/mL lipofectamine. After incubation for 5 hours, the transfection medium was removed, and the cells were placed in complete medium for 48 hours. Relative luciferase activity was determined using the Dual Light reporter gene assay (Perkin Elmer/Tropix, Bedford, MA), per the manufacturer's instructions.

Western blot

We grew UM-SCC 47 and 93-UV-147 cells in 75-cm^2 flasks to 80% confluence, and serum starved them for 24 hours. Whole-cell lysates were made using the radioimmunoprecipitation assay (RIPA) buffer method. Briefly, cells were trypsinized, rinsed, and pelleted at 500 ×g for 2 minutes. The cell pellets were resuspended in RIPA buffer (50 mM Tris-HCl, 150 mM NaCl, 1% NP-40, 0.5% deoxycholic acid, 0.1% SDS, protease inhibitors), vortexed to lyse cells, and debris cleared by centrifugation at 10,000 ×g for 10 minutes at 4°C. Protein concentrations were determined by bicinchoninic (BCA) assay. Proteins were separated in a 10% Tris-HCl polyacrylamide gel (50 μg protein per lane) and transferred to nitrocellulose membrane. Equal protein load was confirmed by staining with Ponceau S (0.1% Ponceau S [w/v] in 5% acetic acid (v/v)). Antibodies to total and phosphorylated p53 were purchased from Cell Signaling Technology (Danvers, MA). β-actin expression was used as the internal loading control.

Quantitative real-time polymerase chain reaction (qRT-PCR)

Briefly, RNA was extracted using Trizol reagent (Life Technologies). Total RNA (1 μg) was reverse-transcribed using a cDNA synthesis kit (Applied Biosystems). Real-time PCR was performed using the Quantitect Sybr green PCR kit (Qiagen), per the manufacturer's instructions, with an Applied Biosystems 7300 real-time PCR system. E6 mRNA sequences were retrieved from the National Center for Biotechnology Information website. The National Center for Biotechnology Information Basic Local Alignment Search Tool (BLAST) server was used to determine primer specificity.

We used the E6 forward primer, CAAACCGTTGTGTGATTTGTTAATTA, and the reverse primer, GCTTTTTGTCCAGATGTCTTTGC. The housekeeping gene 18S (18S Quantitect

Primer Assay, Qiagen) and beta 2-microglobulin were used as the reference gene. Data were analyzed with the comparative C_T method.

Immunofluorescence staining

HPV-positive HNSCC UM-SCC 47 cells grown in chamber slides were treated with 100 ηmol/L of triptolide or DMSO for 24 hours, fixed with 4% paraformaldehyde for 15 minutes at room temperature, permeabilized with 0.1% Triton X-100 for 10 minutes, and then incubated with 1% bovine serum albumin (BSA) at room temperature for 1 hour. Cells were then incubated with a monoclonal anti–p53 antibody at 1:200 dilution overnight at 4°C. After 3 washes (each for 5 minutes) with phosphate-buffered saline, cells were incubated with secondary antibodies: Alexa Fluor 488 conjugated donkey anti-mouse IgG (Molecular Probes) at 1:1200 dilution for 60 minutes at 4°C. The slides were then washed and mounted using Prolong Gold anti-fade agent containing 4′, 6-diamidino-2-phenylindole (DAPI) (Molecular Probes). Immunofluorescence images were obtained on a Nikon Eclipse Ti confocal microscope (Nikon, Melville, NY) using a 60× oil immersion objective. P53 was quantified using ImageJ software (http://rsb.info.nih.gov/ij).

Head and neck carcinoma animal models

To study the effect of Minnelide, a triptolide prodrug, on HPV-positive HNSCC in vivo, we used 2 different animal models. All animal interventions were conducted according to guidelines of the University of Minnesota Institutional Animal Care and Use Committee (IACUC).

The first animal model was a subcutaneous cell injection tumor xenograft. After harvesting of UM-SCC 47 cells, trypan blue exclusion was used to confirm that cells were >90% viable. Cells were resuspended in Matrigel at a concentration of 2,500 cells per μL and kept on ice until injected. Ten female nude mice, 4 to 6 weeks old (Charles River Laboratories), were anesthetized with ketamine (100 mg) and xylazine (10 mg/kg). Then, 200 μL of cell suspension (500,000 cells) were injected subcutaneously into both flanks.

Mice were randomly assigned to a control group or a treated group. Each group developed 10 tumors for analysis. Local tumor development was measured weekly using a caliper. Tumor volumes were calculated using this formula: 0.5 × length × width × depth. The experimental endpoint was the time at which the tumor size reached the maximum tumor burden criterion (set to 2,000 mm^3). Survival was scored when the mice met sacrifice criteria. Once the endpoint was reached, the mice were euthanized and necropsy performed. Primary tumors were removed and evaluated for local invasion. Metastasis was evaluated in the regional lymph nodes, lungs, liver, peritoneal cavity, and spleen.

The second animal model was a patient-derived tumor xenograft. De-identified human HPV-positive tumors were obtained fresh from patients undergoing tumor resections, or from biopsy samples of known oropharyngeal HPV-positive tumors. The tumors were then implanted subcutaneously into young adult severe combined immunodeficiency (SCID) mice (Jackson Laboratory, Bar Harbor, ME). When tumor volumes reached 500 mm^3, tumors were dissected and cut into pieces (each 3 to 5 mm^3), which were then

subcutaneously implanted into both flanks of additional SCID mice (n = 20). All mice were randomized and tagged before treatment, and each tumor was measured (as described above). Each day, mice in the treated group received an intraperitoneal injection of Minnelide (0.42 mg/kg); mice in the control group received an intraperitoneal injection of saline solution. Tissue was harvested and stored for further experiments.

TUNEL assay

After completing the animal experiments, we harvested tissue and fixed it in 10% formalin solution followed by 80% ethyl alcohol. Tissue samples were embedded in paraffin blocks. Histologic sections were cut at 5 μm. Slides were stained with hematoxylin and eosin (H&E) and cover-slipped for histologic evaluation. TUNEL staining was performed on formaldehyde-fixed tissue sections using an in situ cell death determination kit (Roche), per the manufacturer's instructions. TUNEL staining was quantified using ImageJ software (http://rsb.info.nih.gov/ij).

Statistical analysis

Values are expressed as the mean ± standard error of the mean (SEM). The significance of the difference between the control group and the treated group, for each experimental test condition, was analyzed by an unpaired Student *t* test. A P value < 0.05 was considered statistically significant.

To perform our statistical analysis, we used GraphPad Prism (GraphPad Software, San Diego, CA). Unless otherwise stated, all cell line experiments were repeated a minimum of 3 times.

Results

Triptolide inhibited cell viability

Triptolide significantly reduced cell viability of 2 head and neck HPV-positive carcinoma cell lines, UM-SCC 47 (Figure 1A) and 93-VU-147 (Figure 1B), in a time- and dose-dependent manner. In addition, it had the same effects in the HPV-positive cervical carcinoma cell line, SiHa (Figure 1B), as well as in another HPV-positive cervical carcinoma cell line, CaSki (data not shown). Triptolide did not significantly decrease HEK viability (Figure 1D).

Triptolide activated caspase 3/7

Triptolide incubation in UM-SCC 47 cells (Figure 2A), 93-VU-147 cells (Figure 2B), and SiHa cells (Figure 2C) resulted in significant caspase 3/7 activation in a time- and dose-dependent manner, as compared with corresponding controls.

Triptolide inhibited transcription of E6

Triptolide significantly decreased the levels of oncoprotein E6 at 6, 12 and 24 hours, as measured by qRT-PCR (Figure 3), as compared with control DMSO-treated cells. HPV-negative UM-SCC 11A cells were used as negative controls (data not show).

Triptolide reactivated wild-type p53

Triptolide at 100 ηM increased p53 phosphorylation at 24 and 48 hours in UM-SCC 47 cells (panel A), CaSki cells (panel B), and 93-VU-147 cells (panel C), as compared with untreated cells (Figure 4A). In HPV-negative UM-SCC 11A cells, which are known to carry a mutated p53, we did not detect p53 phosphorylation (Figure 4A, panel A and B). Total p53 increased in a time-dependent manner in UM-SCC 47 cells (Figure 4B, panel A), CaSki cells (Figure 4B, panel B), and 93-VU-147 cells (Figure 4B, panel C). Figure 4C, panel A demonstrates the lack of p53 activation after triptolide incubation (100ηM) at early time points (4 and 8 hours) or late time points (24 and 48 hours), in UM-SCC-11A cells. As expected triptolide did not increased total p53 in UM-SCC-11A cells after triptolide incubation, Figure 4C, panel B.

Triptolide incubation (100 ηM) for 24 hours significantly increased the promoter gene activity of p53 in UM-SCC 47 and SiHa cells in a dose-dependent manner (Figure 5A).

In UM-SCC 47 cells treated with 100 ηM of triptolide for 24 hours, nuclei stained with DAPI showed an increase in total p53 nuclear staining, as compared with controls (Figure 5B). Total p53 nuclear staining significantly increased in cells treated with triptolide, as compared with controls (Figure 5C).

Minnelide decreased tumor burden in 2 animal models and increased apoptosis in vivo

Tumor progression significantly decreased in UM-SCC 47 xenografts treated with Minnelide, as compared with grafts in mice treated with saline solution (Figure 6, panel A).

In HPV-positive patient-derived tumor xenografts, Minnelide significantly decreased tumor volume and the rate of tumor progression in the second generation of tumors (Figure 6B).

Representative tumor samples showed that mice treated with Minnelide had a significantly higher percent of TUNEL-positive cells than mice treated with saline (Figure 7A and B).

Minnelide reactivated p53 in vivo

We found significant phosphorylation of p53 at serine 15 in mice treated with Minnelide (n = 4), as compared with minimal or no phosphorylation in mice treated with saline (n = 4) (Figure 8). Each line represents an individual tumor.

Discussion

In our study, we demonstrated reactivation of wild-type p53 in HPV-positive HNSCC in vitro and in vivo by triptolide and its prodrug Minnelide. Triptolide decreased transcription of HPV oncoprotein E6, as demonstrated by E6-mRNA decline at 6 and 12 hours. We also showed that reactivation of wild-type p53 by triptolide in vitro produced a significant decrease in cell viability and remarkable activation of apoptosis in multiple HPV-positive carcinoma cell lines. Triptolide at 50 ηM did not affect viability of normal HEKs; at 100 ηM, it minimally decreased HEK viability. In 2 different HNSCC animal models, Minnelide was effective in decreasing tumor volume and tumor progression. It activated wild-type p53 in vivo, as demonstrated by phosphorylation of p53 at serine 15 in animal tumors.

Collectively, these findings point to the potential therapeutic value of using Minnelide to reactivate wild-type p53 in patients with this devastating disease.

This is the first article to describe activation of wild-type p53 by Minnelide in HPV-positive head and neck carcinoma, leading to significant apoptosis and decreased tumor growth in a preclinical animal model.

Multiple studies have demonstrated the usefulness of targeting E6/E7 in HPV-positive HNSCC.[14,15] The suppression of E6/E7 expression by small molecules leading to reactivation of p53 is a novel and promising approach for treatment of HPV-positive HNSCC. Much remains to learn to further optimize this strategy: the mechanisms by which E6/E7 repression promotes HNSCC cell death are still obscure. Furthermore, in vivo implementation of E6/E7 siRNA and/or shRNA as a treatment strategy could be hampered by multiple factors. Small molecules that target E6/E7 have also been studied, but less extensively.[16-19]

It is well established that HPV E6 oncoprotein facilitates the proteosomal degradation of wild-type p53. For this reason, a viable proposition would be to reactivate wild-type p53 by using small molecules that suppress the function of the HPV viral oncoproteins E6 and E7.

A great quantity of evidence supports the importance of manipulating wild-type p53 signaling as an important factor for cancer treatment. Wild-type p53 interference as a treatment strategy has uncovered the need for specifically reactivating wild-type p53 in cancer tissue, sparing normal body tissues. As a result, the specific reactivation of wild-type p53 in cancer cells would intensify tumor susceptibility to standard radiotherapy and/or chemotherapy.[20]

A number of strategies have been attempted to reactivate wild-type p53. At first, p53 gene therapy was used. Results of phase 2 and 3 clinical trials in patients with advanced-stage HNSCC treated with recombinant adenovirus-p53 (Genedicine) and radiotherapy showed complete regression in 64% of the patients and partial regression in 32%.[21] Although those trials yielded promising results, the main limitations of that approach were safety concerns and inadequate wild-type p53 in vivo administration.

Another strategy has focused on using small molecules to reactivate wild-type p53. Nonpeptide small-molecule compounds Nutlin and RITA (reactivation of p53 and induction of tumor cell apoptosis) have been identified. Nutlin is a potent antagonist of MDM2; RITA prevents p53-MDM2 interaction in vitro and in vivo, inducing massive apoptosis in various cell lines expressing wild-type p53.[22,23]

Still another strategy has involved the dipeptidyl-boronic acid PS-341 (bortezomib), a potent and specific inhibitor of the 26S proteosome. Bortezomib can liberate wild-type p53 from E6, inducing apoptosis and cell cycle arrest in HPV-positive HNSCC.[24] And finally, inhibition of HDM2 Ub ligase activity has been used to restore apoptosis in cancer-expressing wild-type p53.[25,26]

Minnelide is currently being tested in a phase 1 clinical trial for patients with gastrointestinal malignancies. The initial preclinical assessment of Minnelide was completed in tumor-derived animal models of pancreatic cancer; multiple animal models demonstrated the effectiveness of Minnelide in decreasing tumor burden, tumor-associated morbidity, locoregional spread, and in increasing overall survival.[9] Moreover, Minnelide has previously been tested in preclinical pancreatic cancer mouse models.

We previously found no significant changes in serum alanine transaminase (ALT) and aspartate transaminase (AST) levels in animals treated with Minnelide at 0.3 and 0.6 mg/kg for 29 days, as compared with controls. Additionally, animals treated with the same dose of Minnelide used in our current study (0.42 mg/kg) for 385 days did not exhibit an adverse phenotype.

We hypothesize that Minnelide specifically reactivates p53 because of the presence of oncogenic protein E6, not as a general upregulator of p53 limiting Minnelide toxicity.

Although the results of our study are encouraging, a potential limitation was our use of only 2 HPV-positive HNSCC cell lines. Also, although we demonstrated a correlation between the downregulation of E6 oncoprotein and the reactivation of wild-type p53, the specific mechanism by which Minnelide exerts its antitumor effects remains to be determined. Moreover, our patient-derived tumor xenograft model was limited by its reliance on the host's deficient immune system to allow tumor growth.

In conclusion, we found that triptolide and Minnelide caused cell death in vitro and in vivo in HPV-positive HNSCC by reactivating wild-type p53 and thus inducing apoptosis. In addition, in 2 HPV-positive HNSCC animal models, Minnelide decreased tumor progression and induced apoptosis. This study opens the potential of developing Minnelide into an effective chemotherapy agent against HPV-positive HNSCC and lays the foundation for further evaluation of its mechanism of action against HPV-positive HNSCC.

Acknowledgments

We thank Mary Knatterud, PhD, who provided help with editing the article.

References

1. Chaturvedi AK, Engels EA, Pfeiffer RM, et al. Human papillomavirus and rising oropharyngeal cancer incidence in the United States. J Clin Oncol. 2011; 29:4294–4301. [PubMed: 21969503]
2. Gillison ML, Broutian T, Pickard RK, et al. Prevalence of oral HPV infection in the United States, 2009-2010. JAMA. 2012; 307:693–703. [PubMed: 22282321]
3. Brinker AM, Ma J, Lipsky PE, Raskin I. Medicinal chemistry and pharmacology of genus Tripterygium (Celastraceae). Phytochemistry. 2007; 68:732–766. [PubMed: 17250858]
4. Tengchaisri T, Chawengkirttikul R, Rachaphaew N, Reutrakul V, Sangsuwan R, Sirisinha S. Antitumor activity of triptolide against cholangiocarcinoma growth in vitro and in hamsters. Cancer Lett. 1998; 133:169–175. [PubMed: 10072166]
5. Shamon LA, Pezzuto JM, Graves JM, et al. Evaluation of the mutagenic, cytotoxic, and antitumor potential of triptolide, a highly oxygenated diterpene isolated from Tripterygium wilfordii. Cancer Lett. 1997; 112:113–117. [PubMed: 9029176]

6. Phillips PA, Dudeja V, McCarroll JA, et al. Triptolide Induces Pancreatic Cancer Cell Death via Inhibition of Heat Shock Protein 70. Cancer Research. 2007; 67:9407–9416. [PubMed: 17909050]
7. Chen Y-W, Lin G-J, Chia W-T, Lin C-K, Chuang Y-P, Sytwu H-K. Triptolide exerts anti-tumor effect on oral cancer and KB cells in vitro and in vivo. Oral oncology. 2009; 45:562–568. [PubMed: 19359213]
8. Antonoff MB, Chugh R, Borja-Cacho D, et al. Triptolide therapy for neuroblastoma decreases cell viability in vitro and inhibits tumor growth in vivo. Surgery. 2009; 146:282–290. [PubMed: 19628086]
9. Chugh R, Sangwan V, Patil SP, et al. A preclinical evaluation of Minnelide as a therapeutic agent against pancreatic cancer. Science translational medicine. 2012; 4:156ra–139.
10. Velagapudi, M.; Crowell, B. [Accessed November,12 2013 2013] A Phase 1, Multi-Center, Open-Label, Dose-Escalation, Safety, Pharmacokinetic, and Pharmacodynamic Study of Minnelide™ Given Daily for 21 Days Followed by 7 Days Off Schedule in Patients With Advanced GI Tumors. Sep 5. 2013 Available at: http://clinicaltrials.gov/ct2/show/NCT01927965?term=minnelide&rank=1
11. Munoz N, Bosch FX, de Sanjose S, et al. Epidemiologic classification of human papillomavirus types associated with cervical cancer. N Engl J Med. 2003; 348:518–527. [PubMed: 12571259]
12. Munger K, Howley PM. Human papillomavirus immortalization and transformation functions. Virus Res. 2002; 89:213–228. [PubMed: 12445661]
13. el-Deiry WS, Tokino T, Velculescu VE, et al. WAF1, a potential mediator of p53 tumor suppression. Cell. 1993; 75:817–825. [PubMed: 8242752]
14. Ferris RL, Martinez I, Sirianni N, et al. Human papillomavirus-16 associated squamous cell carcinoma of the head and neck (SCCHN): a natural disease model provides insights into viral carcinogenesis. Eur J Cancer. 2005; 41:807–815. [PubMed: 15763658]
15. Rampias T, Sasaki C, Weinberger P, Psyrri A. E6 and e7 gene silencing and transformed phenotype of human papillomavirus 16-positive oropharyngeal cancer cells. J Natl Cancer Inst. 2009; 101:412–423. [PubMed: 19276448]
16. Baleja JD, Cherry JJ, Liu Z, et al. Identification of inhibitors to papillomavirus type 16 E6 protein based on three-dimensional structures of interacting proteins. Antiviral Res. 2006; 72:49–59. [PubMed: 16690141]
17. Divya CS, Pillai MR. Antitumor action of curcumin in human papillomavirus associated cells involves downregulation of viral oncogenes, prevention of NFkB and AP-1 translocation, and modulation of apoptosis. Mol Carcinog. 2006; 45:320–332. [PubMed: 16526022]
18. D'Abramo CM, Archambault J. Small molecule inhibitors of human papillomavirus protein - protein interactions. The open virology journal. 2011; 5:80–95. [PubMed: 21769307]
19. Xie X, Piao L, Bullock BN, et al. Targeting HPV16 E6-p300 interaction reactivates p53 and inhibits the tumorigenicity of HPV-positive head and neck squamous cell carcinoma. Oncogene. 2013
20. Bossi G, Sacchi A. Restoration of wild-type p53 function in human cancer: relevance for tumor therapy. Head Neck. 2007; 29:272–284. [PubMed: 17230559]
21. Pearson S, Jia H, Kandachi K. China approves first gene therapy. Nature biotechnology. 2004; 22:3–4.
22. Vassilev LT, Vu BT, Graves B, et al. In vivo activation of the p53 pathway by small-molecule antagonists of MDM2. Science. 2004; 303:844–848. [PubMed: 14704432]
23. Issaeva N, Bozko P, Enge M, et al. Small molecule RITA binds to p53, blocks p53-HDM-2 interaction and activates p53 function in tumors. Nature medicine. 2004; 10:1321–1328.
24. Li C, Johnson DE. Liberation of functional p53 by proteasome inhibition in human papilloma virus-positive head and neck squamous cell carcinoma cells promotes apoptosis and cell cycle arrest. Cell cycle. 2013; 12:923–934. [PubMed: 23421999]
25. Lai Z, Yang T, Kim YB, et al. Differentiation of Hdm2-mediated p53 ubiquitination and Hdm2 autoubiquitination activity by small molecular weight inhibitors. Proc Natl Acad Sci U S A. 2002; 99:14734–14739. [PubMed: 12407176]
26. Yang Y, Ludwig RL, Jensen JP, et al. Small molecule inhibitors of HDM2 ubiquitin ligase activity stabilize and activate p53 in cells. Cancer cell. 2005; 7:547–559. [PubMed: 15950904]

Abbreviations

HNSCC	head and neck squamous cell carcinoma
HR-HPV	high-risk human papillomavirus
OPSCC	oropharyngeal squamous cell carcinoma
STS	staurosporine
UM-SCC	University of Michigan squamous cell carcinoma

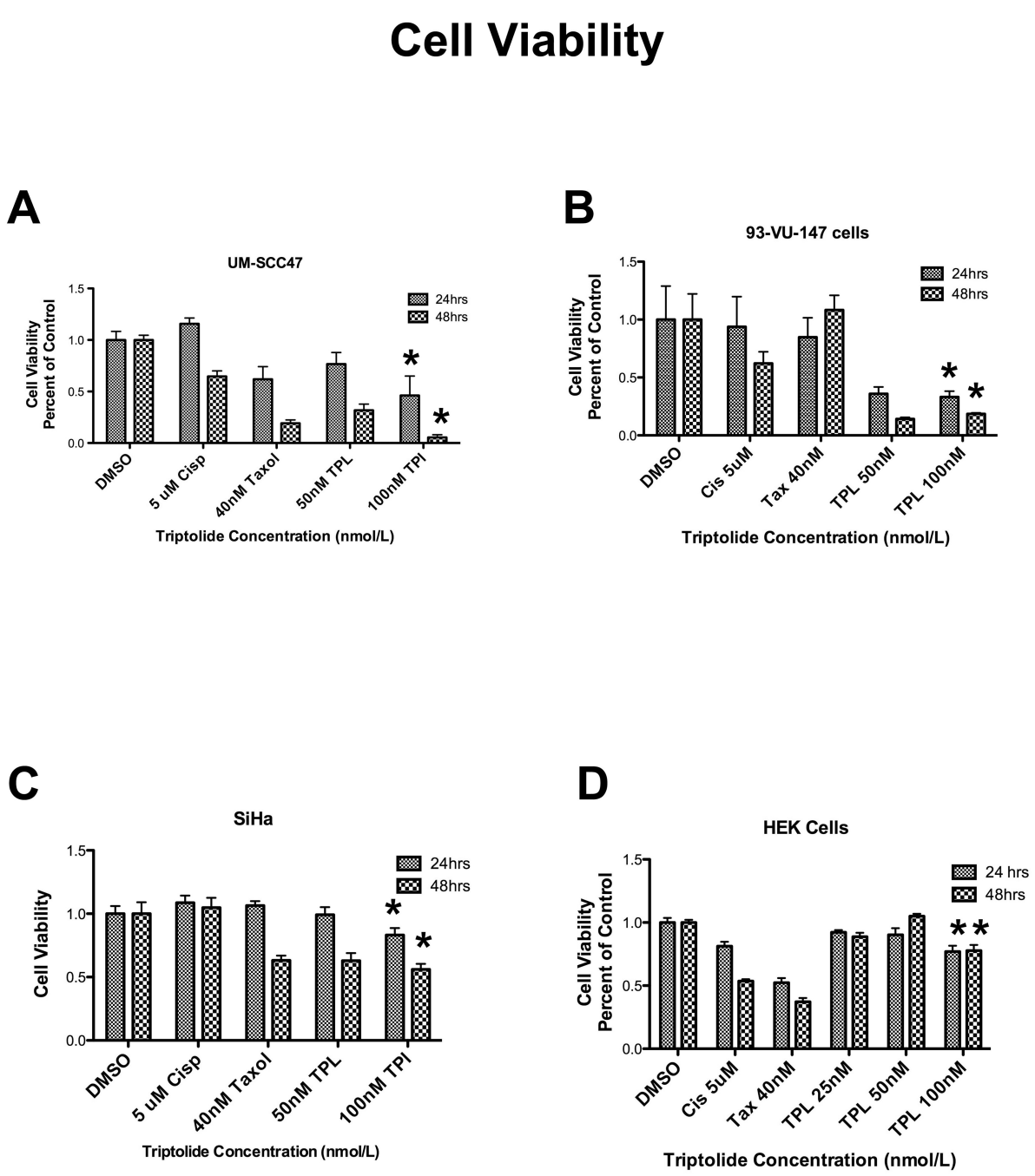

Figure 1. Effect of triptolide on cell viability

Triptolide incubation for 24 and 48 hours significantly decreased cell viability, in a dose-dependent manner (25-100 ηM), in these 3 human papillomavirus (HPV)-positive carcinoma cell lines: **(A)** University of Michigan squamous cell carcinoma (UM-SCC) 47 (n = 3, $P < 0.0001$* for 24 and 48 hours), **(B)** 93-VU-147 (n = 3, $P < 0.0298$* for 24 hours and $P < 0.0118$ for 48 hours), and **(C)** SiHa (n = 3, $P < 0.0014$*), as compared with control cell lines incubated with dimethyl sulfoxide (DMSO). **(D)** Interestingly, triptolide did not significantly decrease cell viability in the human epidermal keratinocyte (HEK) cell line.

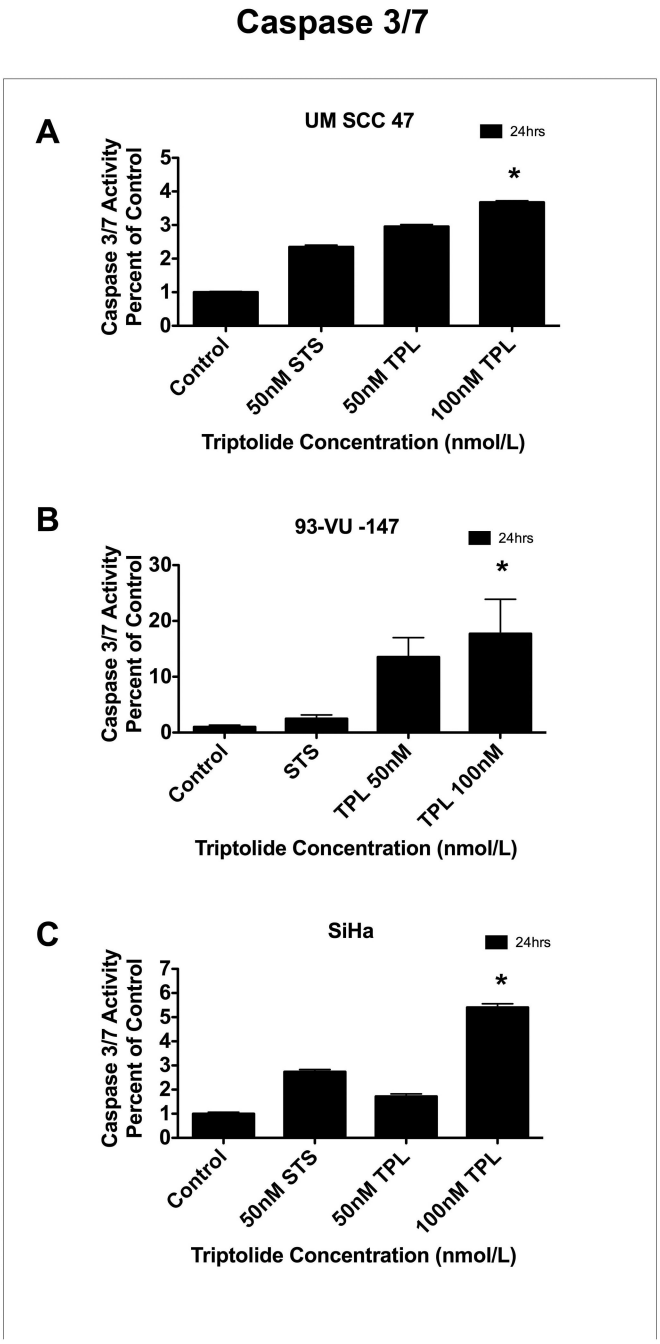

Figure 2. Effect of triptolide on caspase 3/7 activity

Triptolide incubation significantly increased caspase 3/7 activity, in a time-dependent (12 and 24 hours) and dose-dependent (5-100 ηM) manner, in these 3 human papillomavirus (HPV)-positive carcinoma cell lines: **(A)** University of Michigan squamous cell carcinoma (UM-SCC) 47 (n = 3, $P < 0.0001$* for 24 hours), **(B)** 93-VU-147 (n = 3, $P < 0.0003$* for 24 hours), and **(C)** SiHa (n = 3, $P < 0.0001$* for 24 hours), as compared with control cell lines incubated with dimethyl sulfoxide (DMSO). The same effects were observed at 12 hours (data not shown).

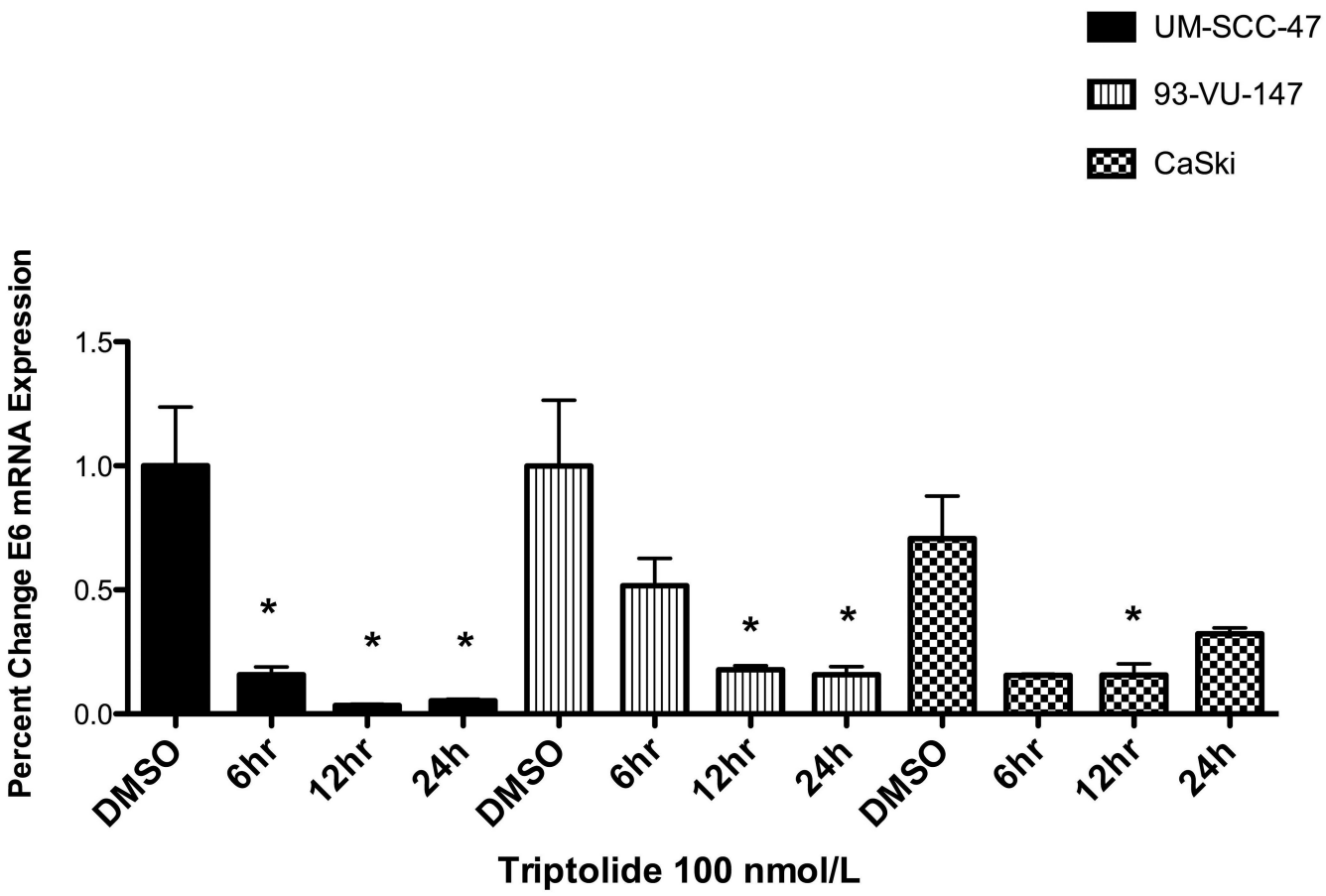

Figure 3. Effect of triptolide on E6 transcription

Triptolide incubation (100 ηM) significantly decreased E6 messenger ribonucleic acid (mRNA), in a time-dependent (6-24 hours) manner, in these 3 human papillomavirus (HPV)-positive carcinoma cell lines: **(A)** University of Michigan squamous cell carcinoma (UM-SCC) 47 (n = 3, P< 0.0243* for 6h; *P* < 0.0149* for 12 h and P< 0.0161* for 24h), **(B)** 93-VU-147 (n = 3, *P* < 0.0373* for 12 h; P< 0.0341* for 24h), and **(C)** CaSki (n = 3, *P* < 0.0497* for 12 hours) and significant decreased linear trend by 1way-ANOVA (n=3, P< 0.0281) .

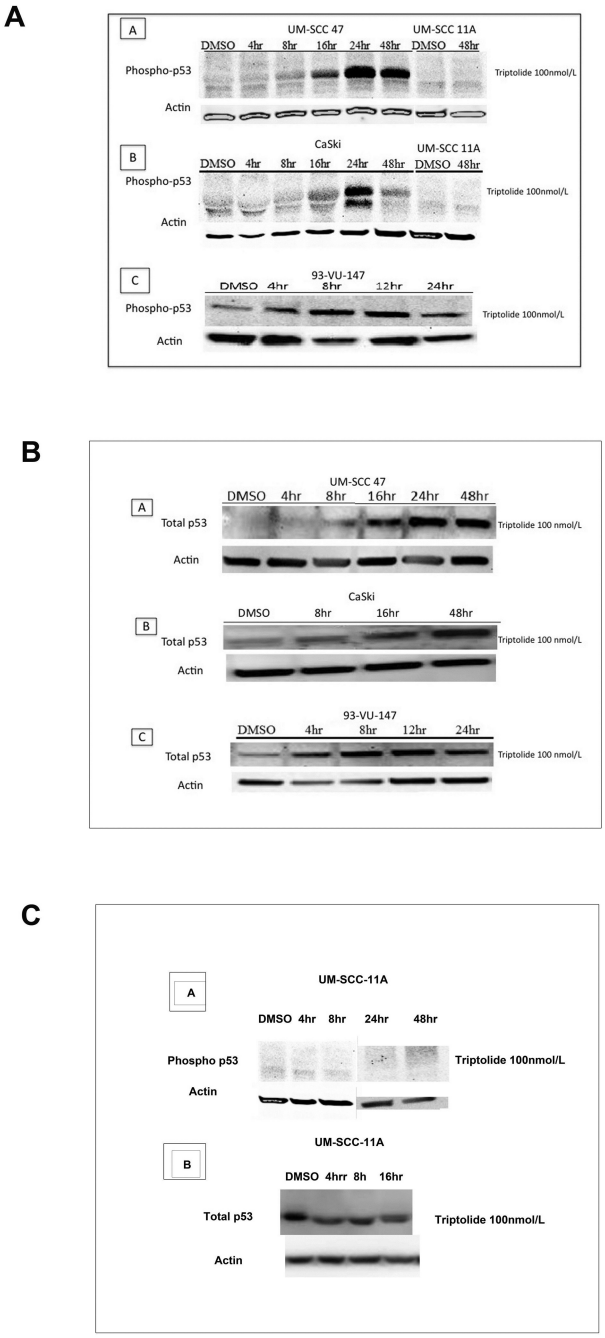

Figure 4. Effect of triptolide on wild-type p53

In a time-dependent manner, triptolide incubation (100 ηM) significantly increased **(a)** phosphorylation of p53 at serine 15 and significantly increased **(b)** total p53 in these 3 human papillomavirus (HPV)-positive carcinoma cell lines: **(A)** University of Michigan squamous cell carcinoma (UM-SCC) 47, **(B)** CaSki, and **(C)** 93-VU-147, as compared with control cell lines incubated with dimethyl sulfoxide (DMSO). No phosphorylation of p53 at serine 15 (4-48 hrs) or increased total p53 (4-16hrs) was observed in the negative HPV cell line UM-SCC-11A **(c)**

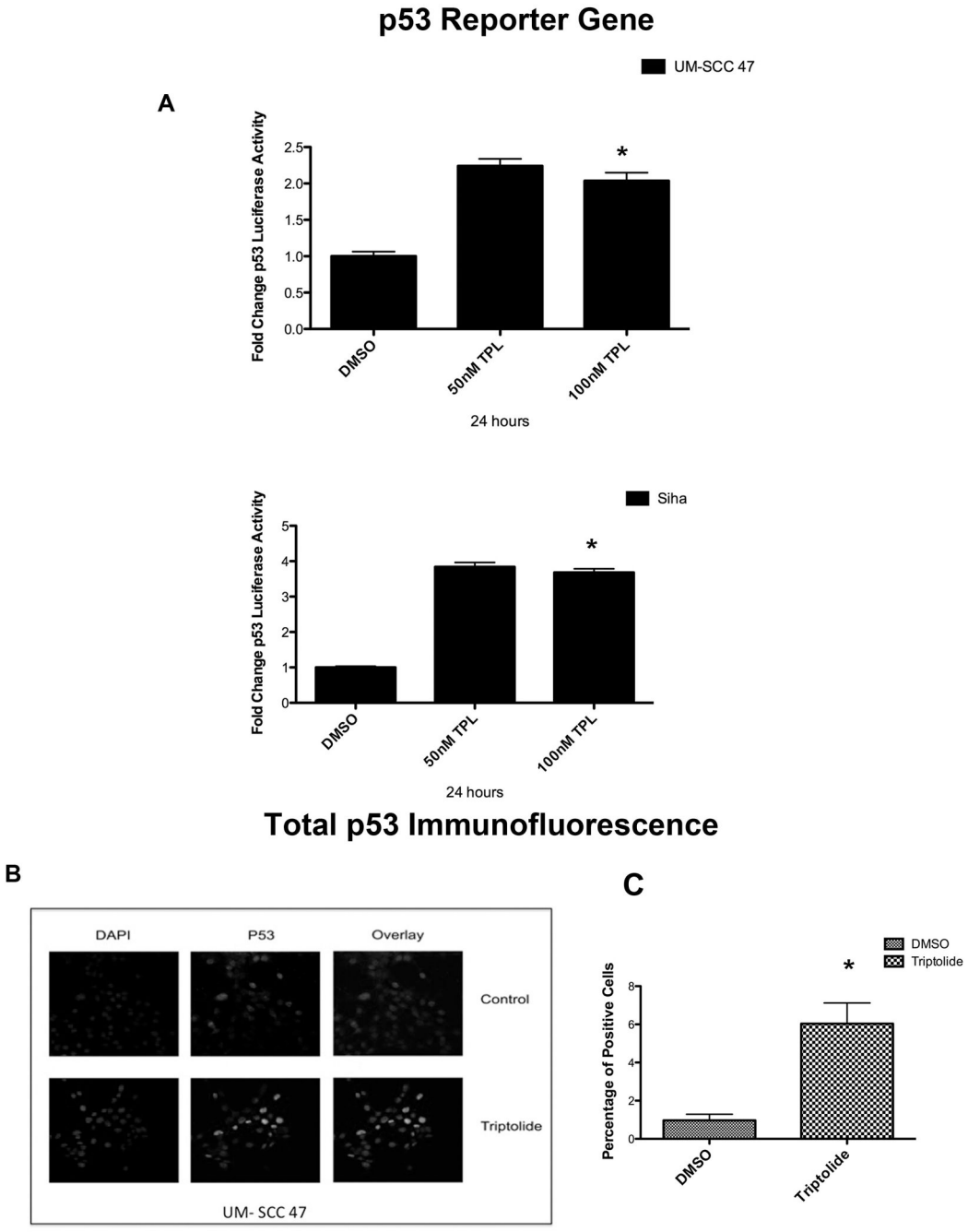

Figure 5. Effect of triptolide on p53 promoter activity and nuclear total p53. (A) Triptolide incubation (50-100 ηM) for 24 hours significantly increased p53 luciferase activity in both the University of Michigan squamous cell carcinoma (UM-SCC) 47 cell line (n = 3, at 50ηM P < 0.0001; at 100ηM P < 0.0002*) and the SiHa cell line (n = 3, *P* < 0.0001* for both concentrations). **(B)** Increased nuclear staining of total p53, per immunofluorescence staining, in the UM-SCC 47 cell line after triptolide treatment. The quantification, per immunofluorescence staining, of triptolide-treated cells as compared with

control cell lines incubated with dimethyl sulfoxide (DMSO) (n = 3, $P < 0.0032$*) is shown in **(C)**.

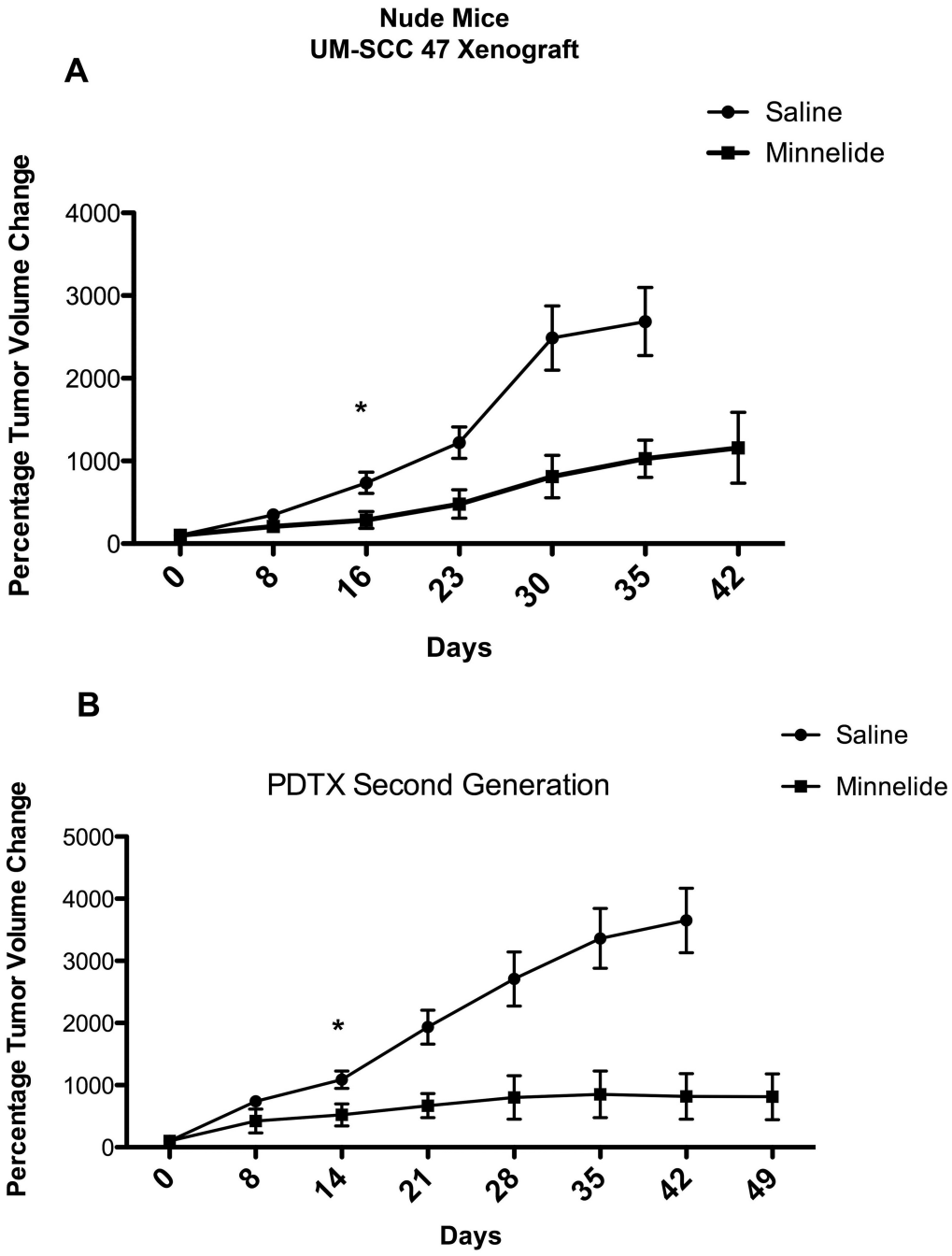

Figure 6. Effect of Minnelide on tumor progression in 2 different xenograft mouse models. (A) In the **cell injection xenograft model,** Minnelide significantly decreased tumor progression, as compared with the saline control group. Statistically difference starts at 16 days ($P <$ 0.0126*) and is sustained through out the experiment. **(B)** In the **patient-derived tumor xenograft model,** Minnelide significantly decreased tumor progression, as compared with the saline control group beginning at day 14 ($P < 0.0176$*) and sustained to the end of the experiment.

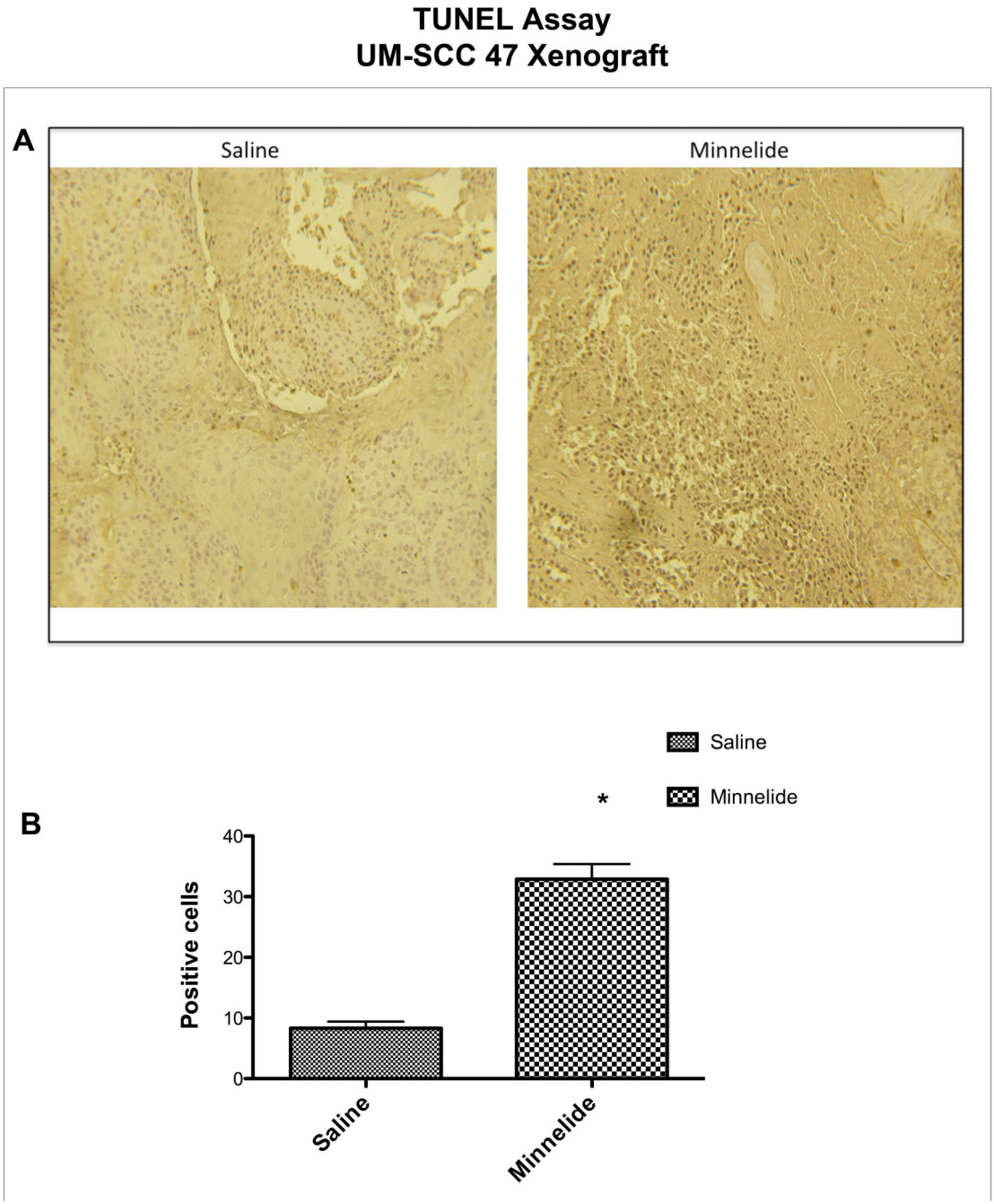

Figure 7. Effect of Minnelide on apoptosis in vivo. (A)

Terminal deoxynucleotidyl transferase dUTP biotin nick end labeling (TUNEL) staining showed that Minnelide increased the number of apoptotic cells, as compared with the control group. The quantification, per TUNEL staining, of Minnelide-treated cells as compared with the control group ($P < 0.0001$*) is shown in **(B)**.

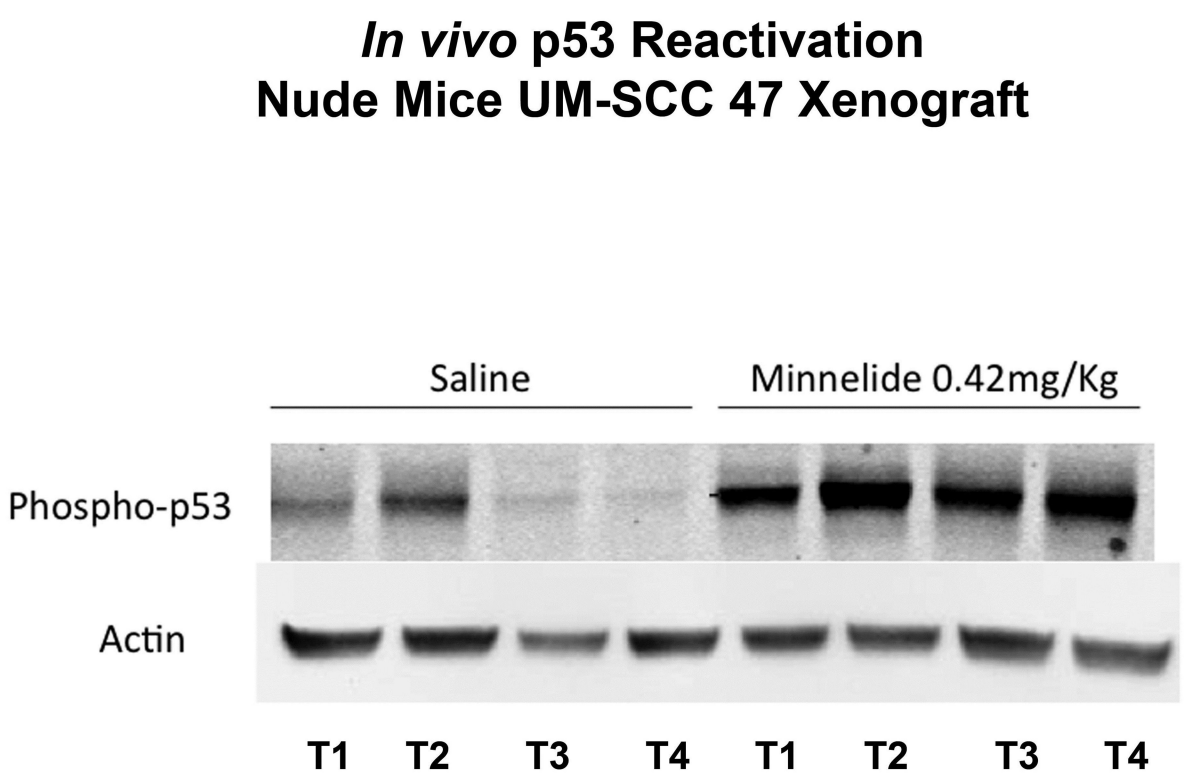

Figure 8. Effect of Minnelide on p53 in vivo

Minnelide increased p53 phosphorylation at serine 15 as compared with the control group.